

Moving Metallic Slab Illuminated by a Plane Wave: Theory and Numerical Analysis Using the Finite Difference Time Domain Method

Mohammad Marvasti and Halim Boutayeb*

Abstract—The response of a uniformly moving metallic slab to an electromagnetic plane wave, at normal incidence, is studied. The analysis is based on the application of boundary conditions to Maxwell's equations as a function of time. The Doppler effect and amplitude of the obtained reflected wave agree with the literature. Moreover, a transferred wave which has not been analyzed in the literature is demonstrated. The frequency shift and the amplitude of this wave are studied analytically with the same technique used for the reflected wave. The transfer of electromagnetic wave through the metallic slab is made possible by the presence of a static magnetic field inside the moving metallic slab, if the motion of the slab is opposite to the direction of propagation of the incident wave. The amplitude of the transferred wave is approximately $2v/c$ times the amplitude of the incidence wave, with v being the speed of motion and c the speed of light in vacuum. This amplitude is thus very small for non-relativistic speeds. The analytical results are validated by full-wave simulations based on the Finite Difference Time Domain method, where both reflected and transferred waves are demonstrated. Furthermore, numerical electric field and magnetic field distributions are presented at different time instants.

1. INTRODUCTION

The problem of reflection and transmission of electromagnetic waves by moving mediums is of important interest and has been extensively investigated in the literature. In [1–5], problems of two moving mediums parallel with the interface are studied thoroughly. In [6–9], the reflection and refraction of normal or obliquely incident electromagnetic wave from a moving dielectric half-space are investigated. In [10], modified forms of Snell's law for refraction from a moving medium illuminated by a plane wave at arbitrary direction are obtained. A three-dimensional solution of the electromagnetic jump conditions at a moving boundary is derived in [11]. In [12], closed-form expressions for the frequencies and wave vectors of reflection and refraction by moving interfaces are presented. A discussion about several questions which arise in obtaining and utilizing boundary conditions along moving interfaces is presented in [13]. In [14], the reflected wave from an expanding dielectric slab is investigated. Power reflection and transmission coefficients are calculated for a moving plasma slab, illuminated by a plane wave source at normal incidence in [15]. The scattered waves by a cylinder moving uniformly and illuminated by a plane wave are discussed in [16]. A technique for boundary movement in Transmission Line Matrix (TLM) networks is described in [17]. Several authors have studied the Doppler effect for a wave reflected from a moving metallic surface. In [18], it is shown that Lorentz's transformations can be derived from the analysis of the reflection of light by a moving mirror. Formulas of the Doppler shift

Received 11 April 2023, Accepted 10 July 2023, Scheduled 19 July 2023

* Corresponding author: Halim Boutayeb (halim.boutayeb@uqo.ca).

The authors are with the Department of Electrical Engineering, University of Quebec, 101 Rue Saint-Jean Bosco, Gatineau (Qc) J8X 3X7, Canada.

for different directions of motion of the mirror and for different incidence angles of the plane wave are presented in [19–23]. In [24, 25], electromagnetic wave scattering from different moving metallic objects is considered.

In this work, the response of a uniformly moving metallic slab to an electromagnetic plane wave, at normal incidence, is studied analytically and numerically. The proposed theoretical analysis is based on energy conservation, the study of a moving plane wave source, and the application of boundary conditions. The Doppler effect and amplitude of the obtained reflected wave agree with the literature. Furthermore, it is shown that part of the wave is transferred on the other side of the slab due to the presence of a static magnetic field inside the moving metallic slab, if the motion of the slab is opposite to the direction of propagation of the incident wave. The proposed analysis is validated by a full-wave numerical investigation based on the Finite Difference Time Domain (FDTD) method with moving structures. The implementation of motion in FDTD is based on the techniques described in [26], which are valid for non-relativistic speeds. In [26], FDTD is used to study the response of a moving inclined dielectric half-space to an electromagnetic plane wave. The results presented in this paper are also valid for non-relativistic speeds. In [26], results for high speeds are presented only for comparing numerical and analytical results or for increasing the Doppler effect in order to obtain a better visualization in the field distribution. In practical applications, only problems with non-relativistic speeds should be considered with the proposed direct FDTD approach [26].

The remainder of the paper is structured as follows. Section 2 shows the study of the Doppler frequency shift and amplitude of the electric and magnetic fields in time and frequency domains for a moving plane wave source. Section 3 presents a theoretical analysis of the amplitudes and frequencies of the transferred and reflected electric and magnetic fields in the frequency and time domains for a moving metallic slab. The theoretical analysis is validated by full-wave simulations in Section 4. Finally, concluding remarks are given in Section 5.

2. MOVING PLANE WAVE SOURCE

The analysis presented in this section will be used in the next section. A plane wave source is moving in $-\vec{x}$ direction, away from the observer, with the speed v , and the observer is at rest as shown in Fig. 1. We used, as the excitation source, a windowed Sine signal $E_{zi}(t) = A_{E_{zi}(t)} \Pi(\frac{t}{N}) \sin(2\pi f_0 t)$, presenting a modulated sinusoid $\hat{E}_{zi}(f) = A_{\hat{E}_{zi}(f)} \frac{N}{f_0} \text{Sinc}(\frac{f-f_0}{N f_0})$ spectrum, where f_0 is the frequency of excitation, and N is the number of periods of Sine function considered for simulation. $A_{E_{zi}(t)}$ and $A_{\hat{E}_{zi}(f)}$ are the amplitudes of incident electric field component in z -axis, in time domain and frequency domain, respectively. This excitation provides a sharp frequency spectrum and makes frequency identification accurate and simple. The observer measures E'_z and E_z , the electric field component in z -axis for moving source and for source at rest, respectively. We call f' the frequency of observed waves when the source

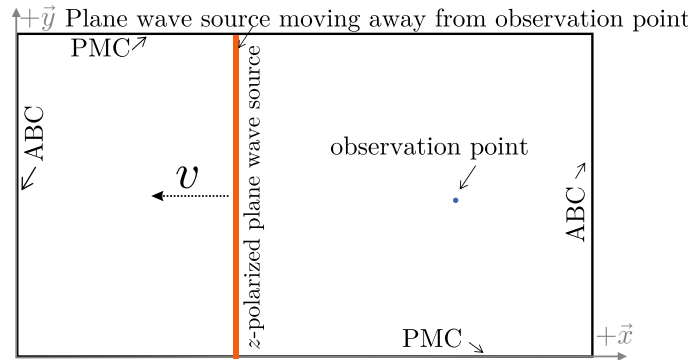


Figure 1. Plane wave source moving away from observation point (FDTD). Absorbing Boundary Conditions (ABCs), Perfect Magnetic Conductors (PMCs), and Perfect Electric Conductors (PECs) are used for the boundaries. PECs are used in the boundaries that are not shown in the figure.

is moving, and f is the frequency when the source is at rest. $A'_{\hat{E}_z(f)}$ and $A'_{E_z(t)}$ are the amplitudes of observed electric field component in z -axis, in the frequency and time domains, respectively, when the source is moving. $A_{\hat{E}_z(f)}$ and $A_{E_z(t)}$ are the same amplitudes when the source is at rest. $A'_{\hat{H}_y(f)}$ and $A'_{H_y(t)}$ are the amplitudes of magnetic field component in y -axis, in the frequency and time domains, respectively, when the source is moving. $A_{\hat{H}_y(f)}$ and $A_{H_y(t)}$ are the same amplitudes when the source is at rest.

Figure 2 shows the simulated FDTD signal received by the observer, in time domain, for different values of v/c , with c being the speed of light in vacuum. Fig. 3 shows spectrum of observed signal. Fig. 4 shows that the simulated frequencies and amplitudes in frequency domain agree with the non-relativistic Doppler effect formula for moving source:

$$\frac{f'}{f} = \frac{A'_{E_z(t)}}{A_{E_z(t)}} = \frac{A'_{H_y(t)}}{A_{H_y(t)}} = \frac{1}{1 + \frac{v}{c}} \tag{1}$$

From Fig. 3 we have:

$$\frac{A'_{\hat{E}_z(f)}}{A_{\hat{E}_z(f)}} = \frac{A'_{\hat{H}_y(f)}}{A_{\hat{H}_y(f)}} = 1 \tag{2}$$

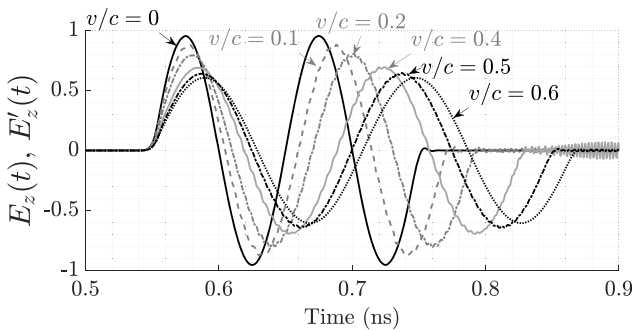


Figure 2. Simulated (FDTD) signal in time domain for plane wave source moving with speed v in normal direction away from observer, for different values of $\frac{v}{c}$.

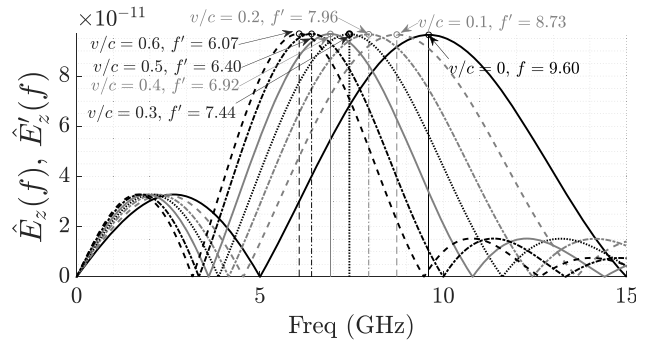


Figure 3. Simulated (FDTD) signal in frequency domain for plane wave source moving with speed v in normal direction away from observer, for different values of $\frac{v}{c}$.

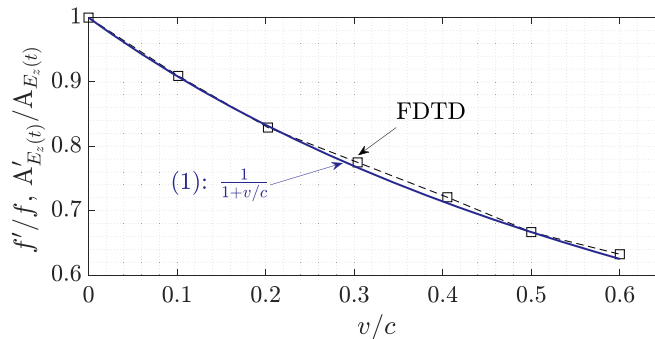


Figure 4. Simulated (FDTD) and predicted Doppler frequency shift and amplitude of the electric field in time domain for plane wave source moving with speed v away from observer, versus $\frac{v}{c}$.

3. THEORETICAL ANALYSIS OF A MOVING METALLIC SLAB

A metallic slab, which is modeled as a Perfect Electric Conductor (PEC), is moving in $-\vec{x}$ direction with the speed v and is illuminated by a plane wave as shown in Fig. 5. The plane wave source is made of a plane of z -polarized current sources. The plane wave is propagating with the speed c in $+\vec{x}$ direction.

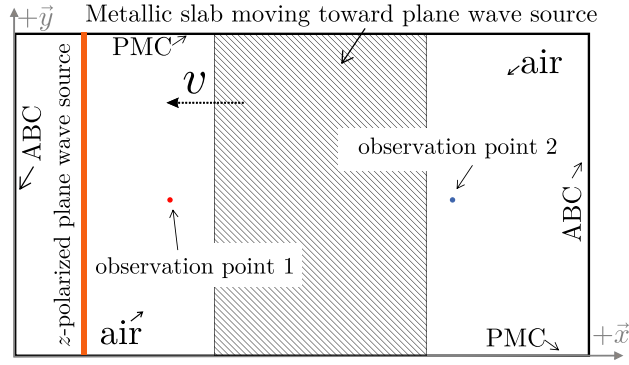


Figure 5. Metallic slab moving toward a plane wave source (FDTD setup).

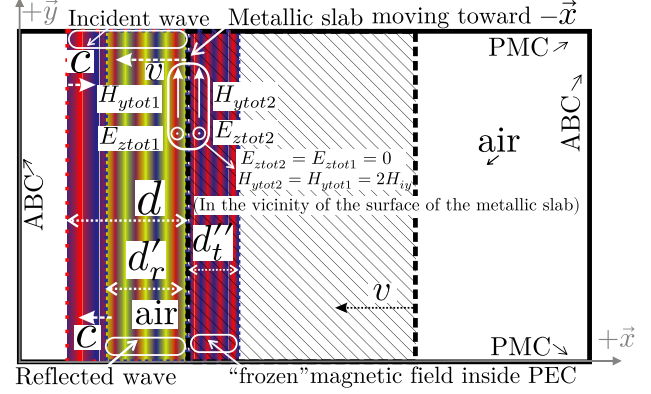


Figure 6. Illumination of a moving metallic slab by a plane wave source. The metallic slab moves toward the plane wave source in $-\vec{x}$ direction. The plane wave propagates in $+\vec{x}$ direction.

3.1. Transferred Wave

Inside the moving metallic slab, all electric field components are equal to zero. In the vicinity of the surface of the metallic slab, the tangential electric field is zero, but the tangential magnetic field is not zero. Because of this, a magnetic field can exist inside the slab when the slab is in motion. In Fig. 6, $E_{z\text{tot}1}$ and $H_{y\text{tot}1}$ are total field components in air. $E_{z\text{tot}2}$ and $H_{y\text{tot}2}$ are total field components inside the metallic slab. For a perfect conductor, in the absence of surface currents, $E_{z\text{tot}1} = E_{z\text{tot}2} = 0$ and $H_{y\text{tot}1} = H_{y\text{tot}2} = 2H_{yi}$ keep true in the vicinity of the surface of the metallic slab, as it moves. H_{yi} is the incident magnetic field. Thus we have $A''_{H_{yt}(t)}/A_{H_{yi}(t)} = 2$, where $A''_{H_{yt}(t)}$ and $A_{H_{yi}(t)}$ are the amplitudes of magnetic field inside the metallic slab and incident magnetic field in \vec{y} direction, respectively.

We call d the distance traveled by the incident signal from a certain point to reach the edge of the slab (Fig. 6). This distance is traveled within time τ :

$$\tau = \frac{d}{c + v} \quad (3)$$

d''_t is the width reached by the magnetic field inside the slab, due to the motion of the slab, within the same time. One can show that:

$$d''_t = v\tau \quad (4)$$

Therefore, the wavelength of the magnetic field, which is “frozen” (not moving) inside the slab ($\lambda_{\text{slabmagn}}$), can be expressed as:

$$\frac{\lambda_{\text{slabmagn}}}{\lambda} = \frac{d''_t}{d} \quad (5)$$

where λ is the wavelength of the incident wave. By substituting (3) and (4) into (5), we obtain:

$$\frac{\lambda_{\text{slabmagn}}}{\lambda} = \frac{v/c}{1 + v/c} \quad (6)$$

The frozen magnetic field remains static as the metallic slab moves toward $-\vec{x}$. When the opposite edge of the slab reaches the static magnetic fields, a transferred wave can start to propagate as illustrated

in Fig. 7 (E_{ztot3} is not null). The opposite edge of the metallic slab acts like a moving plane wave source. By using Huygens' principle [27], the moving slab can be replaced by an equivalent current density $J_{zequiv}^s(t)$ at the location of the slab's second edge. The amplitude of the equivalent current density $J_{zequiv}^s(t)$, named $A'_{J_{zequiv}^s}(t)$, must be chosen such that it generates E_{ztot3} and H_{ytot3} on the right side of the current source in the equivalent problem. This ensures that the boundary condition is satisfied for the moving slab.

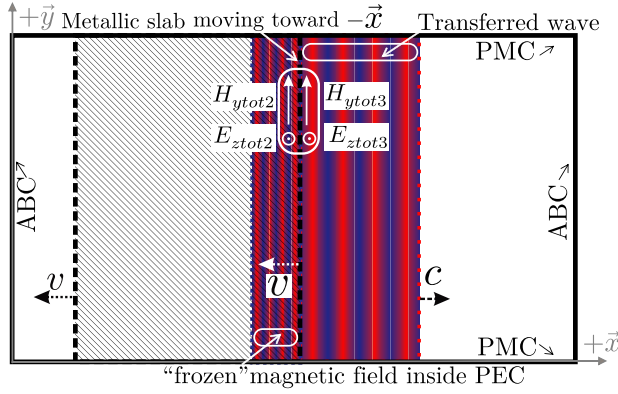


Figure 7. Transferred waves from a moving metallic slab illuminated by a plane wave source. The metallic slab moves toward the plane wave source in $-\vec{x}$ direction.

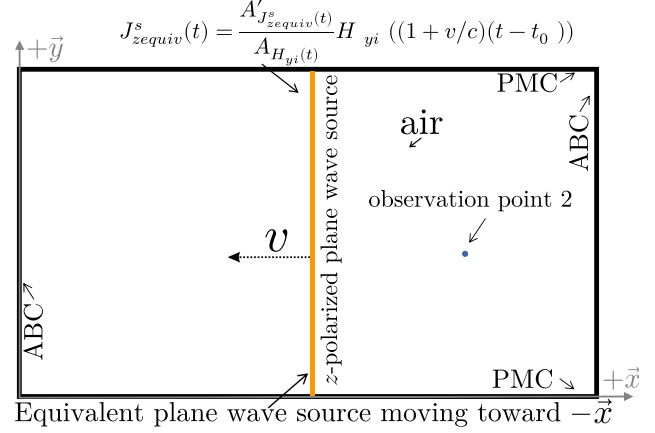


Figure 8. Equivalent problem to analyze the wave on the right-hand side: a plane of current density with amplitude $A'_{J_{zequiv}^s}(t)$ is moving in $-\vec{x}$ direction.

The problem is thus replaced by an equivalent plane wave source that moves with the speed v toward $-\vec{x}$ direction, as illustrated in Fig. 8. In order to obtain the frequency of this equivalent source, one can imagine the static magnetic field inside the slab, as an excitation signal with the wavelength of $\lambda_{slabmagn}$ that is approaching the metallic slab's opposite edge with the speed v . Thus the frequency of excitation signal of equivalent source ($f_{J_{zequiv}^s}$) can be expressed by: $\frac{v}{\lambda_{slabmagn}}$. One can show that the relative frequency is given by:

$$\frac{f_{J_{zequiv}^s}}{f} = \frac{v}{c} \frac{\lambda}{\lambda_{slabmagn}} = 1 + v/c \quad (7)$$

where f is the frequency of the incident wave. Using (7), we have:

$$J_{zequiv}^s(t) = \frac{A'_{J_{zequiv}^s}(t)}{A_{H_{yi}(t)}} H_{yi}((1 + v/c)(t - t_0)) \quad (8)$$

According to Section 2, the observer at rest measures the following relative frequency:

$$\frac{f'_t}{f_{J_{zequiv}^s}} = \frac{1}{1 + v/c} \quad (9)$$

From this, one can obtain:

$$\frac{f'_t}{f} = \frac{f'_t}{f_{J_{zequiv}^s}} \frac{f_{J_{zequiv}^s}}{f} = \frac{1 + v/c}{1 + v/c} = 1 \quad (10)$$

Therefore, the transferred wave has the same frequency as the incident wave. To derive the amplitude of the transferred wave, the ratio of the energy of the frozen magnetic field over the energy of the incident magnetic field in time domain is first expressed as:

$$\frac{\mathbf{W}(H_{ytot2}(t))}{\mathbf{W}(H_{yi}(t))} = \frac{\frac{\mu_0}{2} \int_{-\infty}^{+\infty} |H_{ytot2}(t)|^2 dt}{\frac{\mu_0}{2} \int_{-\infty}^{+\infty} |H_{yi}(t)|^2 dt} = \frac{\int_{-\infty}^{+\infty} \left| 2 \times H_{yi} \left(\left(\frac{1+v/c}{v/c} \right) t \right) \right|^2 dt}{\int_{-\infty}^{+\infty} |H_{yi}(t)|^2 dt} = 4 \times \frac{v/c}{1 + v/c} \quad (11)$$

Now we compute the energy ratio in frequency domain:

$$\frac{\mathbf{W}(\hat{H}_{ytot2}(f))}{\mathbf{W}(\hat{H}_{yi}(f))} = \frac{\frac{\mu_0}{2} \int_{-\infty}^{+\infty} |\hat{H}_{ytot2}(f)|^2 df}{\frac{\mu_0}{2} \int_{-\infty}^{+\infty} |\hat{H}_{yi}(f)|^2 df} = \frac{\int_{-\infty}^{+\infty} \left| \frac{A''_{\hat{H}_{yt}(f)}}{A_{\hat{H}_{yi}(f)}} \times \hat{H}_{yi} \left(\left(\frac{v/c}{1+v/c} \right) f \right) \right|^2 df}{\int_{-\infty}^{+\infty} |\hat{H}_{yi}(f)|^2 df} = \frac{|A''_{\hat{H}_{yt}(f)}|^2}{|A_{\hat{H}_{yi}(f)}|^2} \times \frac{1+v/c}{v/c} \quad (12)$$

where $A''_{\hat{H}_{yt}(f)}$ is the amplitude of the frozen magnetic field in \vec{y} direction inside the slab, and $A_{\hat{H}_{yi}(f)}$ is the amplitude of the incident magnetic field, in frequency domain. By using the Parseval's theorem [28]:

$$\int_{-\infty}^{+\infty} |x(t)|^2 dt = \int_{-\infty}^{+\infty} |\hat{x}(f)|^2 df \rightarrow \frac{\mathbf{W}(\hat{H}_{ytot2}(f))}{\mathbf{W}(\hat{H}_{yi}(f))} = \frac{\mathbf{W}(H_{ytot2}(t))}{\mathbf{W}(H_{yi}(t))} \quad (13)$$

Substituting (11) and (12) into (13), one can obtain:

$$\frac{|A''_{\hat{H}_{yt}(f)}|^2}{|A_{\hat{H}_{yi}(f)}|^2} \times \frac{1+v/c}{v/c} = 4 \times \frac{v/c}{1+v/c} \rightarrow \frac{A''_{\hat{H}_{yt}(f)}}{A_{\hat{H}_{yi}(f)}} = \frac{2v/c}{1+v/c} = 1 - \frac{1-v/c}{1+v/c} \quad (14)$$

By using (2), the amplitude of the transferred magnetic field in frequency domain ($A'_{\hat{H}_{yt}(f)}$) can be derived:

$$\frac{A'_{\hat{H}_{yt}(f)}}{A_{\hat{H}_{yi}(f)}} = \frac{A''_{\hat{H}_{yt}(f)}}{A_{\hat{H}_{yi}(f)}} = 1 - \frac{1-v/c}{1+v/c} = \frac{A'_{\hat{E}_{zt}(f)}}{A_{\hat{E}_{zi}(f)}} \quad (15)$$

$A'_{\hat{E}_{zt}(f)}$ and $A_{\hat{E}_{zi}(f)}$ are the amplitudes of z -polarized transferred and incident electric fields, in frequency domain, respectively. The amplitude of the transferred wave is thus approximately $2v/c$ times of the amplitude of the incidence wave, at first order approximation in terms of v/c . This amplitude is thus very small for non-relativistic speeds. Based on (10), due to the absence of a frequency shift for the transferred wave, the relative amplitude in time domain is equal to the relative amplitude in frequency domain:

$$\frac{A'_{H_{yt}(t)}}{A_{H_{yi}(t)}} = \frac{A'_{\hat{H}_{yt}(f)}}{A_{\hat{H}_{yi}(f)}} = \frac{2v/c}{1+v/c} \quad (16)$$

Also based on (1), the amplitude of the equivalent source can be written:

$$\frac{A'_{J_{zequiv}^s(t)}}{A_{H_{yi}(t)}} = \frac{A'_{J_{zequiv}^s(t)}}{A'_{H_{yt}(t)}} \frac{A'_{H_{yt}(t)}}{A_{H_{yi}(t)}} = (1+v/c) \frac{2v/c}{1+v/c} = 2v/c \quad (17)$$

3.2. Reflected Wave

The wave that is reflected by the first edge of the metallic slab, as shown in Fig. 6, is now considered. At time instant τ , the distance between the wavefront and the edge of the slab, d'_r , can be written:

$$d'_r = c\tau - v\tau = d \frac{c-v}{c+v} \quad (18)$$

where τ is given by (3). The Doppler frequency conversion is thus given by:

$$\frac{f'_r}{f} = \frac{\lambda}{\lambda_{\text{Reflected}}} = \frac{d}{d'_r} = \frac{1+v/c}{1-v/c} \quad (19)$$

where f'_r is the frequency of reflected wave when the metallic slab is moving. The ratio of the energy of reflected wave over the energy of the incident field, in time domain, can be obtained with:

$$\frac{\mathbf{W}(H_{yr}(t))}{\mathbf{W}(H_{yi}(t))} = \frac{\frac{\mu_0}{2} \int_{-\infty}^{+\infty} |H_{yr}(t)|^2 dt}{\frac{\mu_0}{2} \int_{-\infty}^{+\infty} |H_{yi}(t)|^2 dt} = \frac{\int_{-\infty}^{+\infty} \left| H_{yi} \left(\left(\frac{1+v/c}{1-v/c} \right) t \right) \right|^2 dt}{\int_{-\infty}^{+\infty} |H_{yi}(t)|^2 dt} = \frac{1-v/c}{1+v/c} \quad (20)$$

where $H_{yr}(t)$ is the reflected wave in time domain. In the vicinity of the surface of the metallic slab:

$$H_{yr} = H_{y_{tot1}} - H_{yi} = H_{yi} \quad (21)$$

keeps true as it moves. Thus, the amplitude of the reflected wave is equal to the amplitude of the incident wave ($A_{H_{yr}(t)} = A_{H_{yi}(t)}$). The energy ratio in frequency domain is given by:

$$\frac{\mathbf{W}(\hat{H}_{yr}(f))}{\mathbf{W}(\hat{H}_{yi}(f))} = \frac{\frac{\mu_0}{2} \int_{-\infty}^{+\infty} |\hat{H}_{yr}(f)|^2 df}{\frac{\mu_0}{2} \int_{-\infty}^{+\infty} |\hat{H}_{yi}(f)|^2 df} = \frac{\int_{-\infty}^{+\infty} \left| \frac{A'_{\hat{H}_{yr}(f)}}{A_{\hat{H}_{yi}(f)}} \times \hat{H}_{yi} \left(\left(\frac{1-v/c}{1+v/c} \right) f \right) \right|^2 df}{\int_{-\infty}^{+\infty} |\hat{H}_{yi}(f)|^2 df} = \frac{|A'_{\hat{H}_{yr}(f)}|^2}{|A_{\hat{H}_{yi}(f)}|^2} \times \frac{1+v/c}{1-v/c} \quad (22)$$

where $A'_{\hat{H}_{yr}(f)}$ is the amplitude of the reflected wave in frequency domain. By using (13), we have:

$$\frac{|A'_{\hat{H}_{yr}(f)}|^2}{|A_{\hat{H}_{yi}(f)}|^2} \times \frac{1+v/c}{1-v/c} = \frac{1-v/c}{1+v/c} \rightarrow \frac{A'_{\hat{H}_{yr}(f)}}{A_{\hat{H}_{yi}(f)}} = \frac{1-v/c}{1+v/c} = \frac{A'_{\hat{E}_{zr}(f)}}{A_{\hat{E}_{zi}(f)}} \quad (23)$$

where $A'_{\hat{E}_{zr}(f)}$ is the amplitude of the reflected electric field in frequency domain. The result obtained for the reflected wave agrees with the literature and is valid for relativistic speeds. Indeed, the classical wave theory and special relativity predict the same Doppler effect formula for the reflected wave from a moving mirror, at normal incidence. It is interesting to note that the following relationship between the amplitudes of transferred and reflected waves is obtained:

$$\frac{A'_{\hat{E}_{zt}(f)}}{A_{\hat{E}_{zi}(f)}} = 1 - \frac{A'_{\hat{E}_{zr}(f)}}{A_{\hat{E}_{zi}(f)}} \quad (24)$$

which can also be written as $A'_{\hat{E}_{zt}(f)} + A'_{\hat{E}_{zr}(f)} = A_{\hat{E}_{zi}(f)}$. One can state that the solutions obtained for the transferred wave could also be valid for relativistic speeds, because the solutions obtained for the reflected wave are valid at relativistic speeds.

4. FDTD ANALYSIS OF A MOVING METALLIC SLAB

A series of full-wave simulations were carried out in order to validate the previous study, by using the Finite Difference Time Domain method. The FDTD setup is described in Fig. 5.

Two observation points are used to compute the reflected and transferred waves. A windowed Sine excitation is used for a good visualization of the Doppler effect. Fig. 9 shows the simulated amplitude of the reflected wave in frequency domain for different values of $\frac{v}{c}$. An analysis of the amplitude at the peak frequency and of Doppler frequency shift shows that the numerical results agree with the theory. Fig. 10

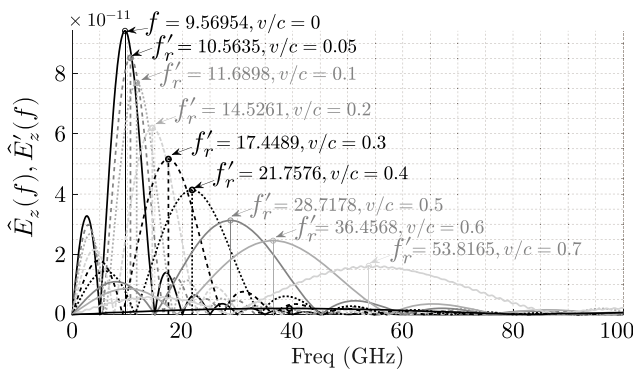


Figure 9. Simulated amplitude of the reflected wave in frequency domain for different values of $\frac{v}{c}$.

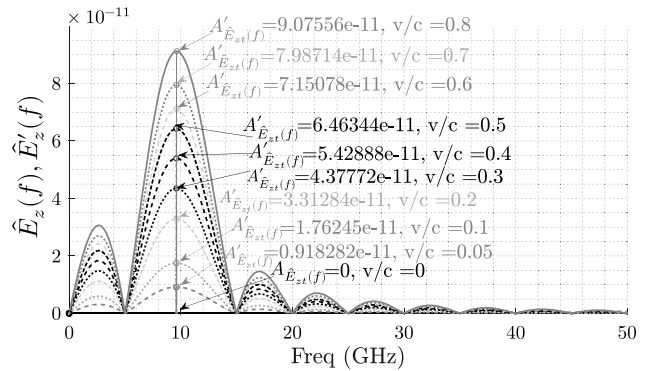


Figure 10. Simulated amplitude of the transferred wave in frequency domain for different values of $\frac{v}{c}$.

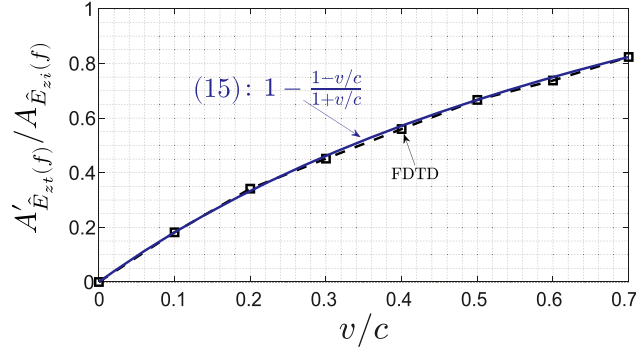


Figure 11. Amplitude of transferred wave versus $\frac{v}{c}$, for metallic slab moving toward $-\vec{x}$ direction.

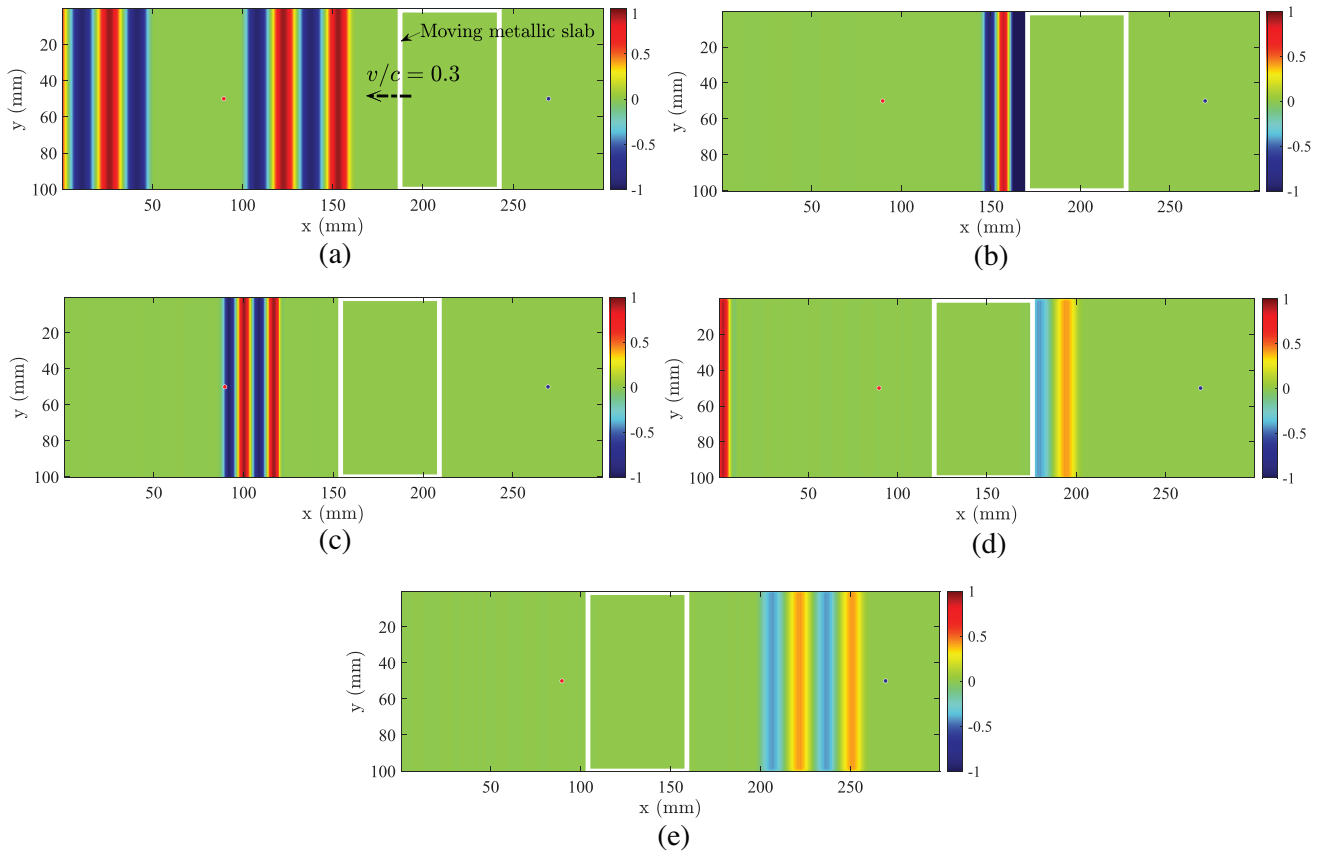


Figure 12. Simulated electric field distribution for a metallic slab moving toward a plane wave source with $\frac{v}{c} = 0.3$, at different time instants. (a) $t = 0.3$ ns, (b) $t = 0.5$ ns, (c) $t = 0.7$ ns, (d) $t = 1.1$ ns, (e) $t = 1.3$ ns.

presents the simulated amplitude of the transferred wave in frequency domain for different values of $\frac{v}{c}$. The numerical results confirm that no Doppler frequency shift is obtained for the transferred wave. Moreover, the amplitude at the peak frequency agrees with the analytical result (15), as shown in Fig. 11.

Figures 12 and 13 show, at different time instants, the electric field and magnetic field distributions, respectively. For a good visualization of the Doppler effect, ratio $\frac{v}{c} = 0.3$ is considered. The edges of the metallic slab are marked with white color. At $t = 0.7$ ns, the reflected wave can be clearly seen in both Fig. 12(c) and Fig. 13(c). Its wavelength is smaller than the incident wave wavelength, as expected. At

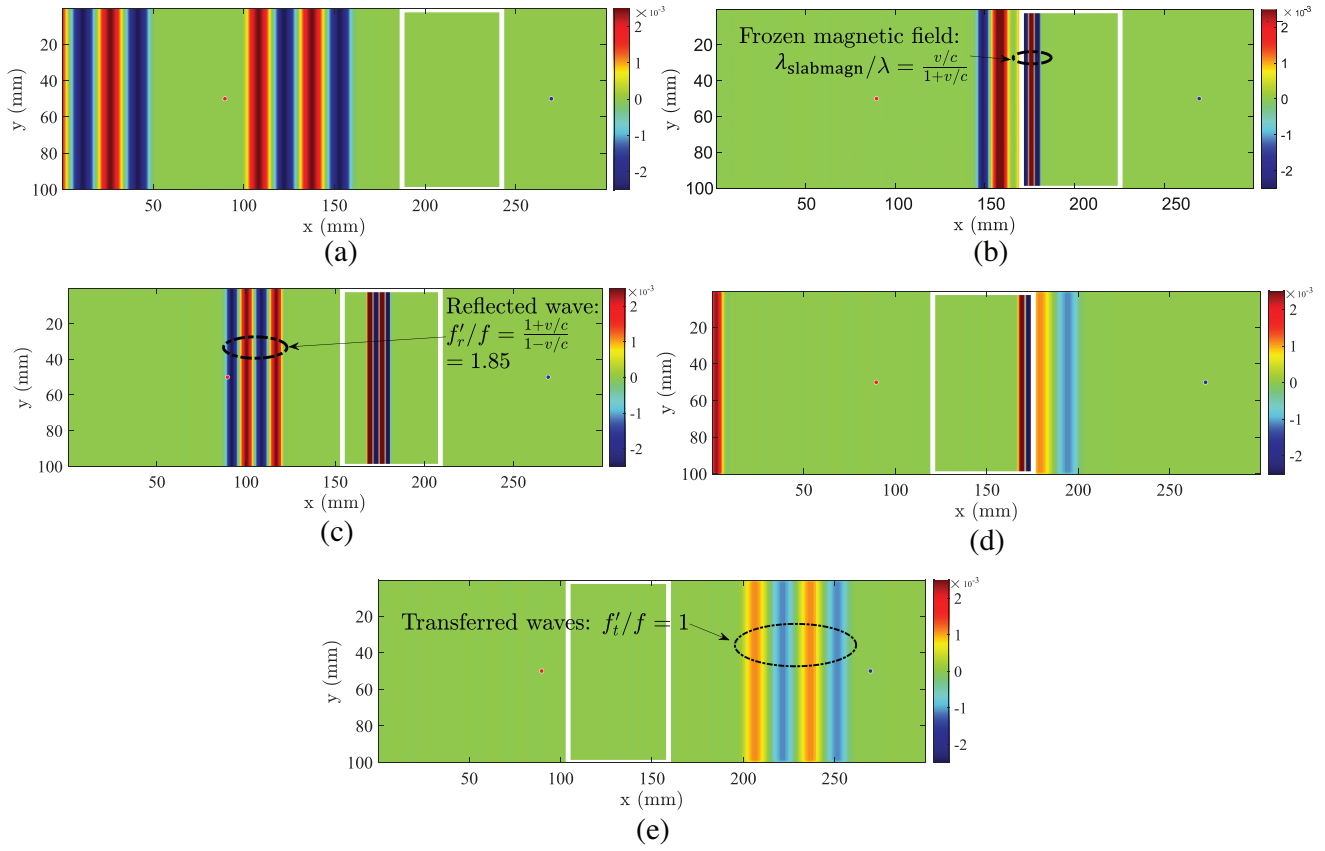


Figure 13. Simulated magnetic field distribution for a metallic slab moving toward a plane wave source with $\frac{v}{c} = 0.3$, at different time instants. (a) $t = 0.3$ ns, (b) $t = 0.5$ ns, (c) $t = 0.7$ ns, (d) $t = 1.1$ ns, (e) $t = 1.3$ ns.

the same time instant, one can observe a magnetic field inside the metallic slab but no electric field. The magnetic field is static, and its wavelength agrees with the previous analysis. At $t = 1.3$ ns, one can observe an electromagnetic wave propagating in $+\vec{x}$ direction at the right-hand side of the slab. The frequency of this transferred wave is the same as the frequency of the incident wave. These full-wave results, which demonstrate the presence of both, the reflected wave studied extensively in the literature and the transferred wave which is analyzed in this paper for the first time, further validate the proposed investigation.

The results presented in this paper agree with experimental results reported in the literature for very fast moving materials. Indeed, in [12], the authors describe the following: “the relative shift of the frequency was then approximately 20% and this was confirmed experimentally” and “no increase in the amplitude on reflection was observed”. The authors then explain that the materials become transparent at very high speeds. This agrees with the analysis presented in this work.

5. CONCLUSION

This paper has presented a new analysis of a uniformly moving metallic slab illuminated by a plane wave, at normal incidence. In addition to the well-known reflected wave, a transferred wave is demonstrated, and new analytical formulas are derived for this wave. The transfer of electromagnetic wave through the metallic slab is made possible by the presence of a static magnetic field inside the moving metallic slab, if the motion of the slab is opposite to the direction of propagation of the incident wave. The proposed study is validated by full-wave simulations based on the Finite Difference Time Domain method. We have verified that the space mesh and time step of the FDTD discretization have no effect on the results.

Moreover, the same results were obtained by replacing the material of the slab from a perfect conductor to a material with high conductivity. Further experiments are needed to verify if the obtained results are not a paradox of Maxwell's equations for a moving metallic object.

This work shows that Maxwell's equations predict the reflected and transferred waves for a moving metallic slab illuminated by a plane wave. There are two main reasons that can explain why the transferred wave has not been studied in the literature, either theoretically or experimentally. First, the amplitude of the transferred wave is very small for non-relativistic speeds (its amplitude is approximately $2v/c$ times of the amplitude of the incidence wave, with v being the speed of motion and c the speed of light in vacuum). Second, the presence of a transferred wave through a moving metallic slab may seem surprising at first. However, it is well known that a magnetic field can be present inside a metallic object.

REFERENCES

1. Yeh, C., "Reflection and transmission of electromagnetic waves by a moving dielectric medium," *Journal of Applied Physics*, Vol. 36, No. 11, 3513–3517, 1965.
2. Shiozawa, T. and K. Hazama, "General solution to the problem of reflection and transmission by a moving dielectric medium," *Radio Science*, Vol. 3, No. 6, 569–575, 1968.
3. Lee, S. and Y. Lo, "Reflection and transmission of electromagnetic waves by a moving uniaxially anisotropic medium," *Journal of Applied Physics*, Vol. 38, No. 2, 870–875, 1967.
4. Tai, C., "The dyadic Green's function for a moving isotropic medium," *Tech. Rep.*, 1964.
5. Tanaka, K. and K. Hazama, "Reflection and transmission of electromagnetic waves by a moving inhomogeneous medium," *Radio Science*, Vol. 7, No. 10, 973–978, 1972.
6. Yeh, C., "Brewster angle for a dielectric medium moving at relativistic speed," *Journal of Applied Physics*, Vol. 38, No. 13, 5194–5200, 1967.
7. Daly, P. and H. Gruenberg, "Energy relations for plane waves reflected from moving media," *Journal of Applied Physics*, Vol. 38, No. 11, 4486–4489, 1967.
8. Pyati, V., "Reflection and refraction of electromagnetic waves by a moving dielectric medium," *Journal of Applied Physics*, Vol. 38, No. 2, 652–655, 1967.
9. Valenzuela, G., "Scattering of electromagnetic waves from a slightly rough surface moving with uniform velocity," *Radio Science*, Vol. 3, No. 12, 1154–1157, 1968.
10. Kong, J.-A. and D. K. Cheng, "Wave behavior at an interface of a semi-infinite moving anisotropic medium," *Journal of Applied Physics*, Vol. 39, No. 5, 2282–2286, 1968.
11. Costen, R. and D. Adamson, "Three-dimensional derivation of the electrodynamic jump conditions and momentum-energy laws at a moving boundary," *Proc. IEEE*, Vol. 53, No. 9, 1181–1196, 1965.
12. Bolotovskii, B. M. and S. N. Stolyarov, "Reflection of light from a moving mirror and related problems," *Sov. Phys. Usp.*, Vol. 32, 813, 1989.
13. Ostrovskii, L. A., "Some moving boundaries paradoxes in electrodynamics," *Radio-Physics Research Institute*, Vol. 116, 315–326, 1975.
14. Pogorzelski, R. J., "Electromagnetic scattering from an expanding dielectric slab," *Journal of Mathematical Physics*, Vol. 11, No. 5, 1685–1689, 1970.
15. Chawla, B. and H. Unz, "Reflection and transmission of electromagnetic waves normally incident on a plasma slab moving uniformly along a magnetostatic field," *IEEE Trans. Antennas Propag.*, Vol. 17, No. 6, 771–777, 1969.
16. Censor, D., "Scattering of electromagnetic waves by a cylinder moving along its axis," *IEEE Trans. Microw. Theory Tech.*, Vol. 17, No. 3, 154–158, 1969.
17. Mueller, U., A. Beyer, and W. Hofer, "Moving boundaries in 2-D and 3-D TLM simulations realized by recursive formulas," *IEEE Trans. Microw. Theory Tech.*, Vol. 40, No. 12, 2267–2271, 1992.
18. Ives, H. E., "The Doppler effect from moving mirrors," *JOSA*, Vol. 30, No. 6, 255–257, 1940.

19. Gjurchinovski, A., "Reflection of light from a uniformly moving mirror," *American Journal of Physics*, Vol. 72, No. 10, 1316–1324, 2004.
20. Gjurchinovski, A., "The Doppler effect from a uniformly moving mirror," *European Journal of Physics*, Vol. 26, No. 4, 643, 2005.
21. He, Q. and Y. Huang, "Reflection of plane electromagnetic waves from the surface of a perfect conductor moving in an arbitrary direction," *Chin. Sci. Bull.*, Vol. 45, 1564–1569, 2000.
22. McWilliams, J., "Electromagnetics: A discussion of fundamentals," *Thought: Fordham University Quarterly*, Vol. 14, No. 4, 677–680, 1939.
23. Ashworth, D. and P. Davies, "The Doppler effect in a reflecting system," *Proc. IEEE*, Vol. 64, No. 2, 280–281, 1976.
24. Abdelazeez, M., L. Peach, and S. Borkar, "Scattering of electromagnetic waves from moving surfaces," *IEEE Trans. Antennas Propag.*, Vol. 27, No. 5, 679–684, 1979.
25. Restricks, R. C., "Electromagnetic scattering by a moving conducting sphere," *Radio Science*, Vol. 3, No. 12, 1144–1154, 1968.
26. Marvasti, M. and H. Boutayeb, "Analysis of moving dielectric half-space with oblique plane wave incidence using the Finite Difference Time Domain method," *Progress In Electromagnetics Research M*, Vol. 115, 119–128, 2023.
27. Smith, G. S., *An Introduction to Classical Electromagnetic Radiation*, Cambridge Univ. Press, 1997.
28. Parseval, M.-A., "Mémoire sur les séries et sur l'intégration complète d'une équation aux différences partielles linéaires du second ordre, à coefficients constants, Mém. prés. par divers savants," *Acad. des Sciences*, Vol. 1, No. 1, 638, Paris, 1806.